

High temperature thick film sensor development based on doped lanthanum chromites refractory semiconductors materials

Javier A. Mena¹, Katarzyna Sabolsky¹, Anthony A. Abrahamian¹, Domenic T. Cipollone¹, Konstantinos Sierros¹, Edward M. Sabolsky¹, Víctor Mendoza-Estrada²

¹Department of Mechanical and Aerospace Engineering,
West Virginia University, Morgantown, WV 26506, USA

²Applied Physics Research Group, Physics Department,
Universidad del Norte, Barranquilla, Colombia

**MS&T'22 Presentation October 12th
Advanced Materials for Harsh Environments**

Introduction

- Processes such as energy generation, metals/glass manufacturing, coal gasification and aerospace technology applications require health and process monitoring in harsh-environments.
- **Harsh-environments conditions include:**
 - ❖ High temperature (500-1800°C)
 - ❖ High pressure (up to 1000 psi)
 - ❖ Corrosive, erosive and reducing environments.
- **Ability to monitor:**
 - ❖ Temperature
 - ❖ Structural stability of systems components
- **US DOE Overall Goal:** Develop health and temperature sensors (and sensor arrays) printed on refractory produced by advanced 2D/3D printing.



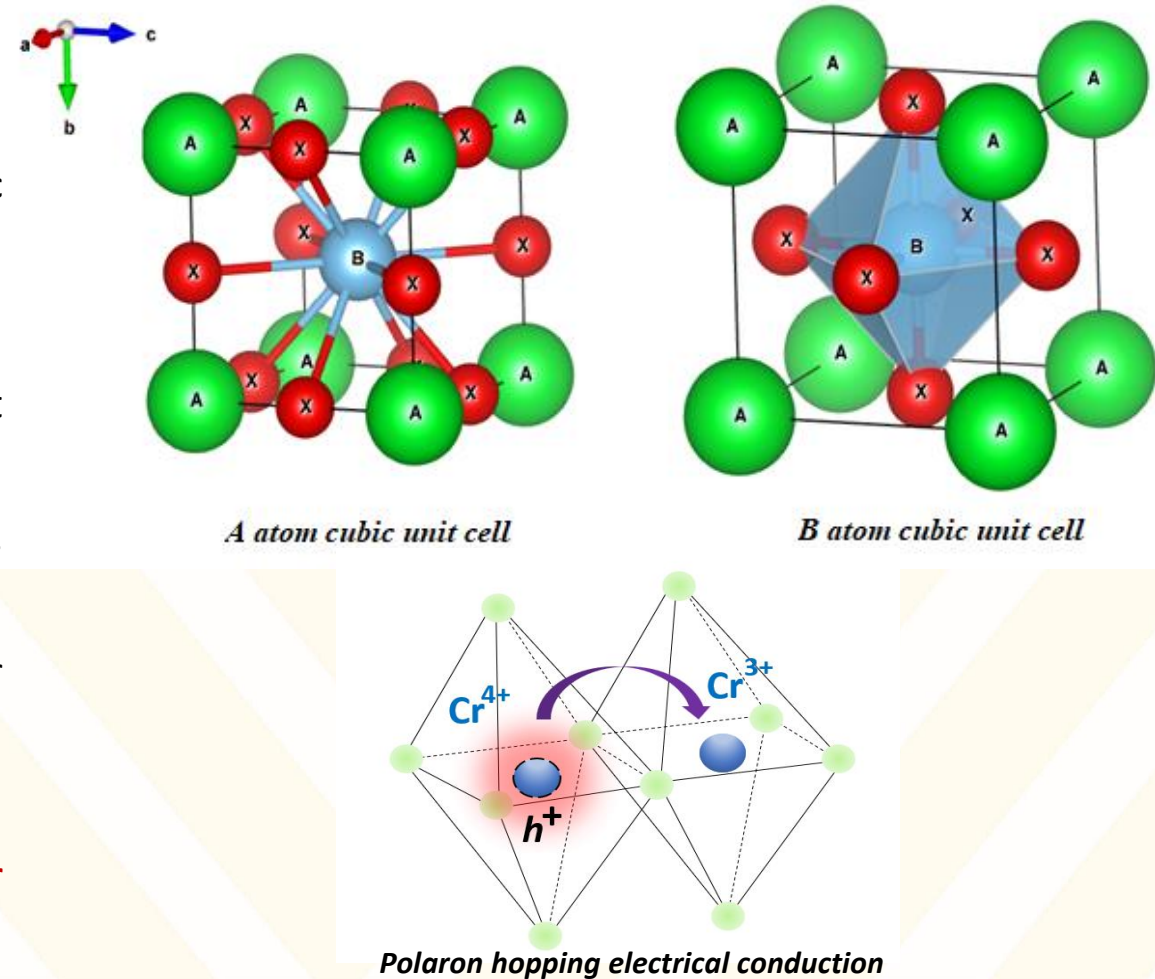
Objectives of This Work

- 1) Synthesize high-temperature refractory LaCrO_3 powders with various p-type doping schemes using the Pechini sol-gel method.
- 2) Characterization phase development/structure (XRD), microstructure and grain size distribution (SEM), optical properties (UV-Vis) and bulk density.
- 3) Study the electrical properties (electrical conductivity and Seebeck coefficient) of compositions at high temperatures conditions and various atmospheres (oxidizing, reducing, different oxygen partial pressures) of these compositions.
- 4) Computational DFT modeling of the LaCrO_3 structure and electrical properties.
- 5) Fabricate surface printed thick-film temperature sensors utilizing these materials and test at high-temperature.

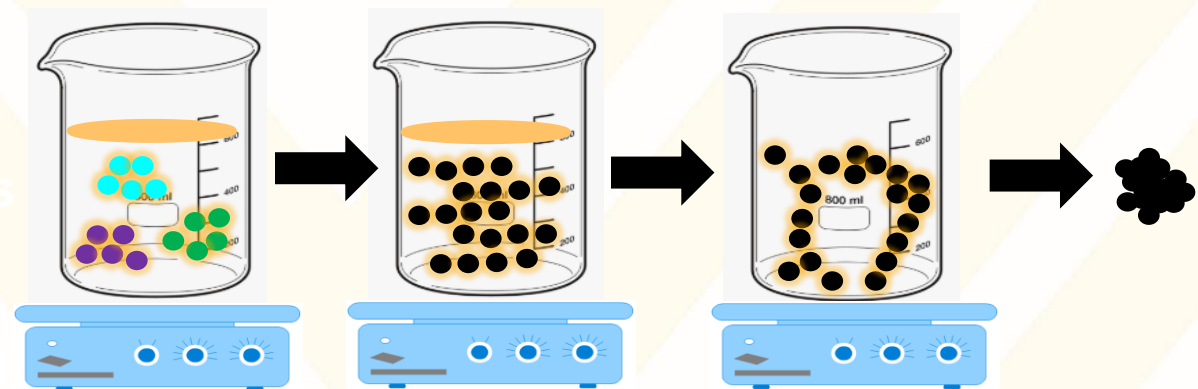
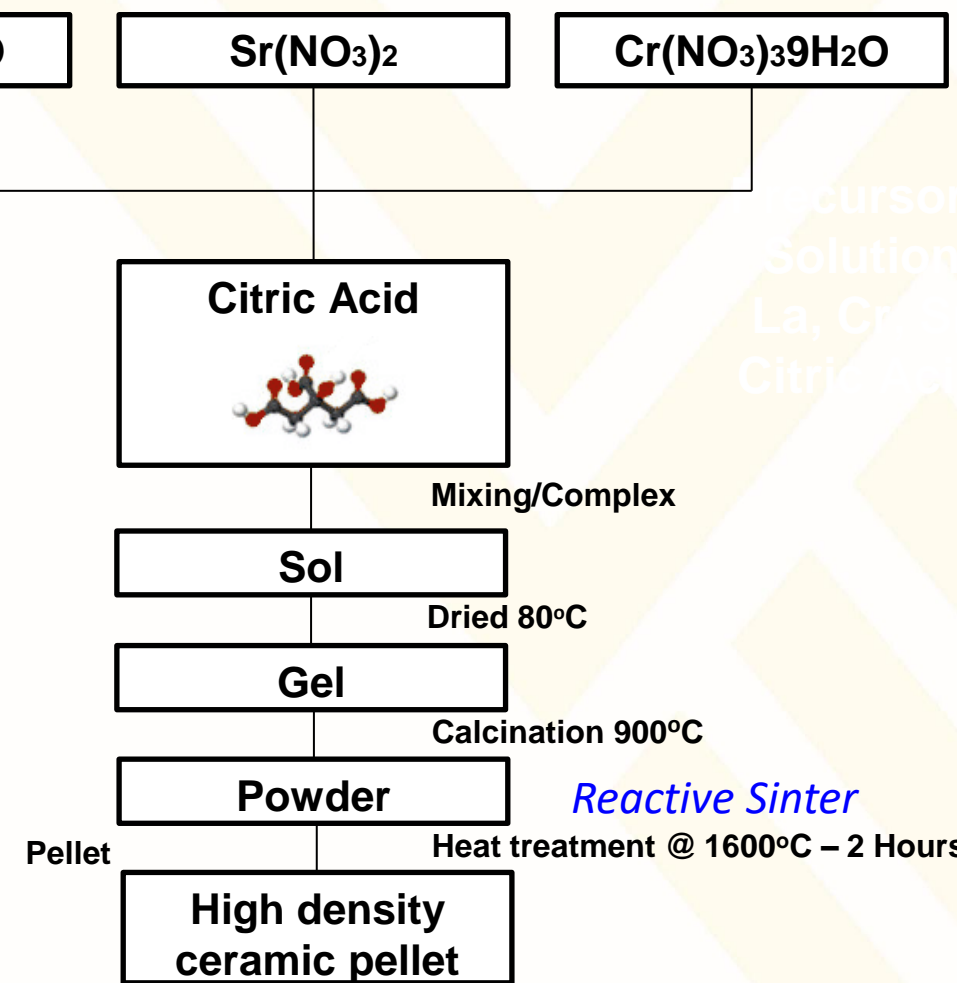
Lanthanum Chromite: General Aspects

- High melting point (~ 2500 °C).
- Chemically stable under oxidative and reducing atmospheres.
- Pure LaCrO_3 shows semiconducting behavior with no to low ionic conduction.
- $\sigma = >10\text{-}100 \text{ S}\cdot\text{cm}^{-1}$ (RT – 1000°C).
- Calcium substitution increase conductivity from 1.0 to 40.0 $\text{S}\cdot\text{cm}^2$ at 1000°C (Mori *et al.* 1997)
- Polaron hopping electrical conductivity mechanism (Webb *et al.* 1977).
- Compatibility (thermal expansion coefficients matching) near refractory materials, $\sim 10 \times 10^{-6} \text{ }^{\circ}\text{C}^{-1}$.

*Electrical properties (mostly in the 1990-2000's) in literature typically shown for <1000 °C due to original focus for Solid-Oxide Fuel Cell (SOFC) applications.



Sol Gel Synthesis and Pellet Fabrication



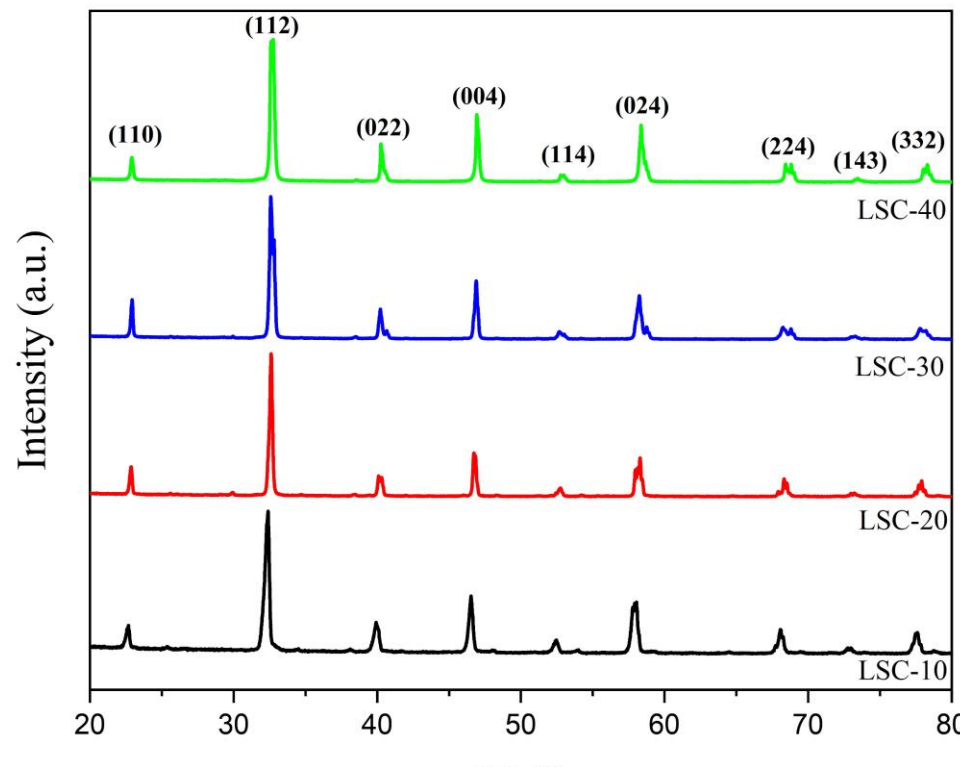
- ✓ Pechini-like process used.
- ✓ High homogenous and adequate sintering.
- ✓ High density (typical in literature <93% density).
- 🚫 Low yields and not easy to scale-up

Compositions Studied:

A-site: $\text{La}_{1-x}\text{Sr}_x\text{CrO}_3$, $\text{La}_{1-x}\text{Ca}_x\text{CrO}_3$
($x = 0.1, 0.2, 0.3, 0.4$)

B-site: $\text{La}_{0.8}\text{Sr}_{0.2}\text{Cr}_{1-y}\text{Mn}_y\text{O}_3$
($y = 0.1, 0.2, 0.3, 0.4$)

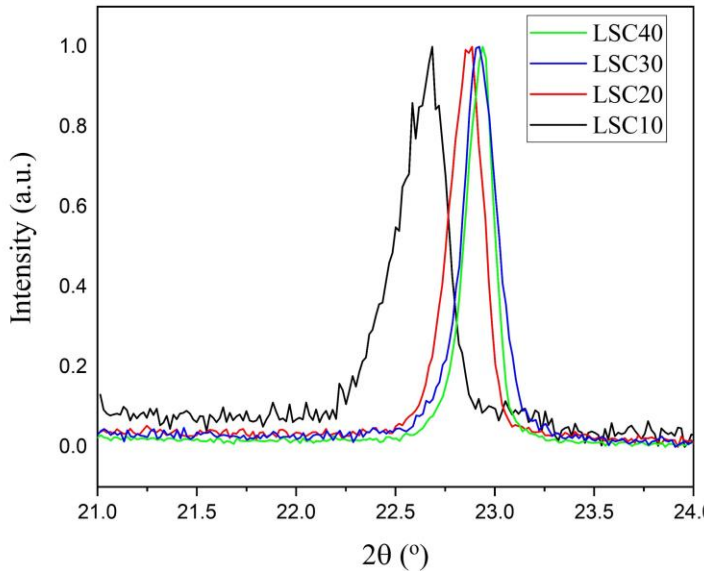
Crystalline Structure/Phase Analysis



X-ray diffractograms for the samples of the
 $\text{La}_{1-x}\text{Sr}_x\text{CrO}_3$ series

- ❖ Single phase doped lanthanum chromites materials were obtained successful (no residual oxide or pyrochlore peaks).
- ❖ Using Pechini Sol-Gel method permitted doped lanthanum chromites at high solubility levels (40%).
- ❖ Solubility limits $>40\%$ substitution level (Sujatha *et al.* 1992).
- ❖ No impurities extra peaks were present in the final prepared powders and ceramic pellets.

Lattice Parameters, Unit Cell Volume and Density

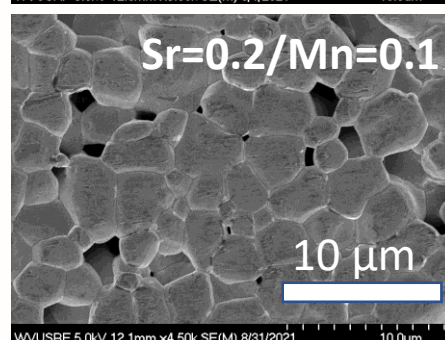
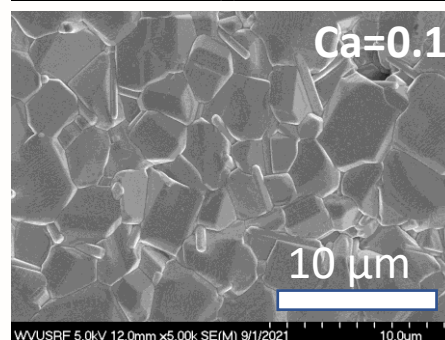
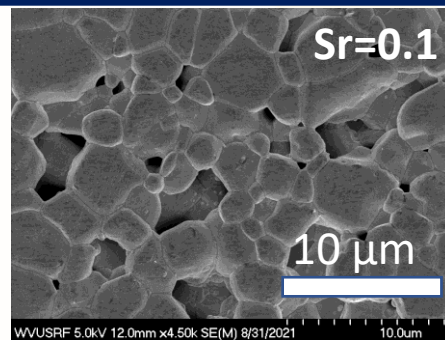


Lattice parameters, unit cell volume and XRD theoretical density for doped lanthanum chromites perovskites

Composition	Lattice parameters (Å)			Volume (Å ³)	$\rho_{XRD\text{Theoretical}}$ (g/cm ³)
	a	b	c		
$\text{La}_{0.9}\text{Sr}_{0.1}\text{CrO}_3$	5.5124	5.5668	7.7926	239.1299	6.4932
$\text{La}_{0.8}\text{Sr}_{0.2}\text{CrO}_3$	5.4988	5.5425	7.7853	237.2747	6.4004
$\text{La}_{0.7}\text{Sr}_{0.3}\text{CrO}_3$	5.4769	5.5233	7.7580	234.6839	6.3259
$\text{La}_{0.6}\text{Sr}_{0.4}\text{CrO}_3$	5.4524	5.5122	7.7407	232.6441	6.2350
$\text{La}_{0.9}\text{Ca}_{0.1}\text{CrO}_3$	5.4180	5.5039	7.7332	230.6050	6.5963
$\text{La}_{0.8}\text{Ca}_{0.2}\text{CrO}_3$	5.4092	5.4982	7.7264	229.7898	6.3341
$\text{La}_{0.7}\text{Ca}_{0.3}\text{CrO}_3$	5.3994	5.4877	7.7058	228.3264	6.0872
$\text{La}_{0.6}\text{Ca}_{0.4}\text{CrO}_3$	5.3897	5.4622	7.6853	226.2520	5.8528
$\text{La}_{0.8}\text{Sr}_{0.20}\text{Cr}_{0.90}\text{Mn}_{0.10}\text{O}_3$	5.4734	5.5648	7.7765	236.8595	6.1533
$\text{La}_{0.8}\text{Sr}_{0.20}\text{Cr}_{0.80}\text{Mn}_{0.20}\text{O}_3$	5.4705	5.5587	7.7702	236.2829	6.1766
$\text{La}_{0.8}\text{Sr}_{0.20}\text{Cr}_{0.70}\text{Mn}_{0.30}\text{O}_3$	5.4598	5.5398	7.7498	234.4020	6.2344
$\text{La}_{0.8}\text{Sr}_{0.20}\text{Cr}_{0.60}\text{Mn}_{0.40}\text{O}_3$	5.4146	5.4981	7.7065	229.4225	6.3783

- ❖ Decrease in lattice parameters (and volume) were observed when dopant cations is introduced in the lattice.
- ❖ To achieve neutrality chromium change from Cr^{+3} to Cr^{+4} , reduction in the chromium size occurs (Hyun Choi *et al.* 2013) .

Microstructure/Grain Size Distribution



Average grain size and bulk density distribution for $\text{La}_{1-x}\text{Sr}_x\text{CrO}_3$, $\text{La}_{1-x}\text{Ca}_x\text{CrO}_3$ series

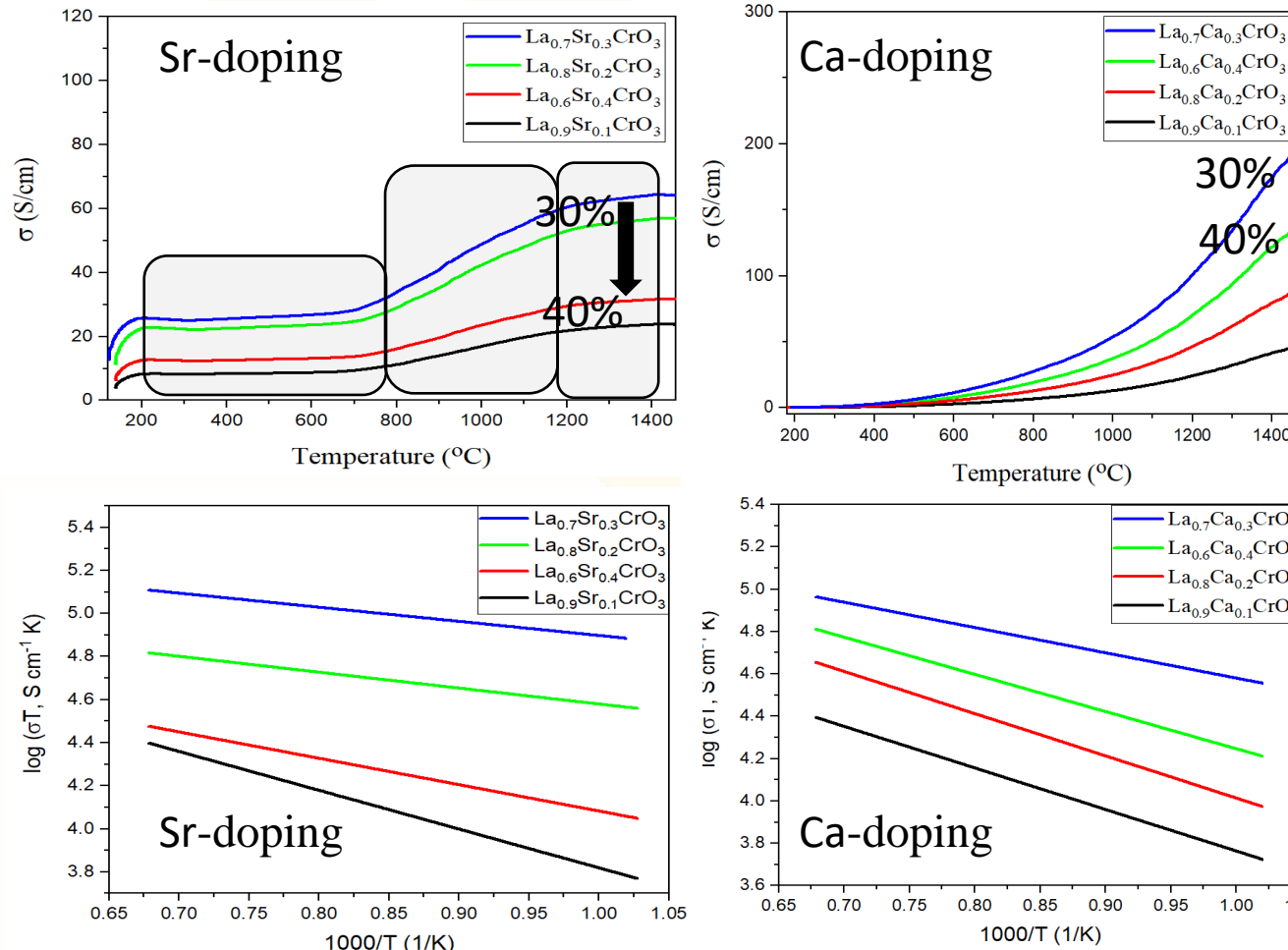
Composition	Average Grain Size (μm)	Relative Percentage Bulk Density (%)
$\text{La}_{0.9}\text{Sr}_{0.1}\text{CrO}_3$	3.6	94
$\text{La}_{0.8}\text{Sr}_{0.2}\text{CrO}_3$	3.5	95
$\text{La}_{0.7}\text{Sr}_{0.3}\text{CrO}_3$	3.6	95
$\text{La}_{0.6}\text{Sr}_{0.4}\text{CrO}_3$	3.2	94
$\text{La}_{0.9}\text{Ca}_{0.1}\text{CrO}_3$	4.1	96
$\text{La}_{0.8}\text{Ca}_{0.2}\text{CrO}_3$	3.7	97
$\text{La}_{0.7}\text{Ca}_{0.3}\text{CrO}_3$	3.7	97
$\text{La}_{0.6}\text{Ca}_{0.4}\text{CrO}_3$	3.6	98

$\% \text{Sr} \uparrow$

$\% \text{Ca} \uparrow$

- ❖ Pechini Sol Gel prepared calcium, strontium, manganese doped lanthanum chromite powders exhibit better sinterability and densification under oxidizing conditions (undoped $\downarrow 90\%$).
- ❖ The samples of Ca doped lanthanum chromite powder have more dense microstructures. Furthermore, it was found that the incorporation of Ca, Sr in the A site of the lanthanum chromite increases grain growth (undoped $< 3 \mu\text{m}$).

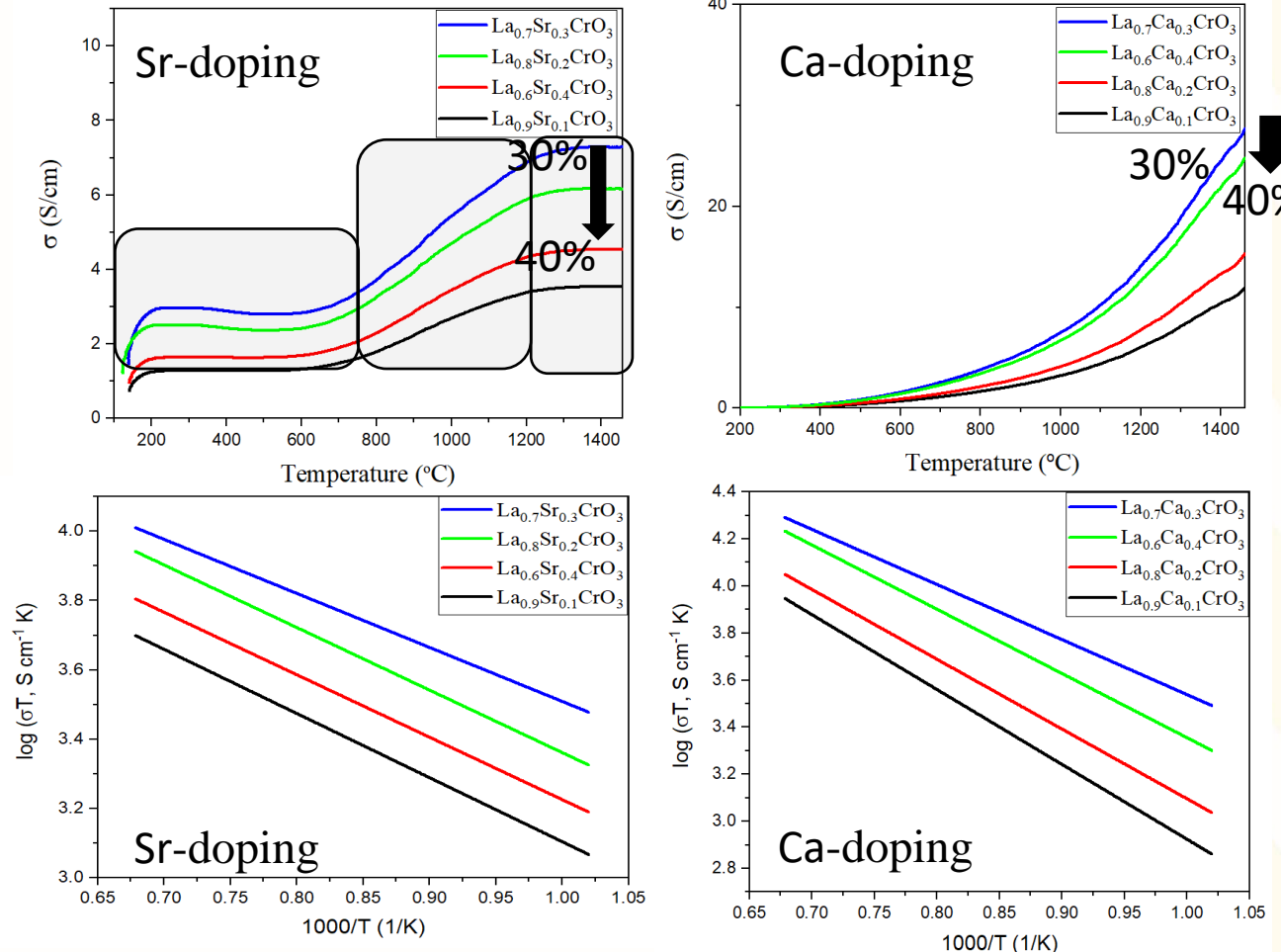
DC Electrical Conductivity (Oxidizing Atmosphere)



Electrical conductivity vs temperature and Arrhenius Plot $\text{La}_{1-x}\text{Sr}_x\text{CrO}_3$, $\text{La}_{1-x}\text{Ca}_x\text{CrO}_3$

- ❖ Conductivity typically exponentially increases with increase in carrier mobility, but 30 to 40% all drop in conductivity (believe slight second phase or higher lattice strain).
- ❖ Sr doped shows three regions, not seen in literature, since most tests $<850\text{--}1000\text{ }^\circ\text{C}$. (believe V_o at high temperature)
- ❖ Arrhenius relationship fits for higher temperature regimes.
- ❖ Calcium doped compositions present higher conductivity due the lower distortion effects on lattice structure.

DC Electrical Conductivity (Reducing Atmosphere)



- ❖ Conductivity decrease for all temperature range under reducing atmosphere ($\text{H}_2 5\%/\text{N}_2 95\%$).
- ❖ Under reducing conditions, oxygen vacancies form to keep neutrality (drop in hole carrier concentration).
- ❖ Sr conductivity still displays regions of altered mechanism.
- ❖ All compositions present lower conductivity as dopant increases (but still 40% lower than 30% in all cases).

Electrical conductivity vs temperature and Arrhenius Plot for $\text{La}_{1-x}\text{Sr}_x\text{CrO}_3$, $\text{La}_{1-x}\text{Ca}_x\text{CrO}_3$

DC Electrical Conductivities/Activation Energies

Composition	Air Atmosphere		Reducing Atmosphere	
	Conductivity @ 1000°C (S/cm)	Activation energy (eV)	Conductivity @ 1000°C (S/cm)	Activation energy (eV)
La _{0.9} Sr _{0.1} CrO ₃	16.672	0.1552	2.691	0.3238
La _{0.8} Sr _{0.2} CrO ₃	42.882	0.1427	4.572	0.2597
La _{0.7} Sr _{0.3} CrO ₃	49.032	0.1055	5.534	0.1719
La _{0.6} Sr _{0.4} CrO ₃	23.599	0.1498	3.462	0.3102
La _{0.9} Ca _{0.1} CrO ₃	13.211	0.1417	3.152	0.3240
La _{0.8} Ca _{0.2} CrO ₃	24.170	0.1298	4.118	0.2103
La _{0.7} Ca _{0.3} CrO ₃	52.823	0.1028	7.602	0.1367
La _{0.6} Ca _{0.4} CrO ₃	38.152	0.1175	6.626	0.1747

$$\sigma = \frac{\sigma_0}{T} \exp\left(\frac{-\Delta E_a}{kT}\right)$$



Slope $\propto E_a$

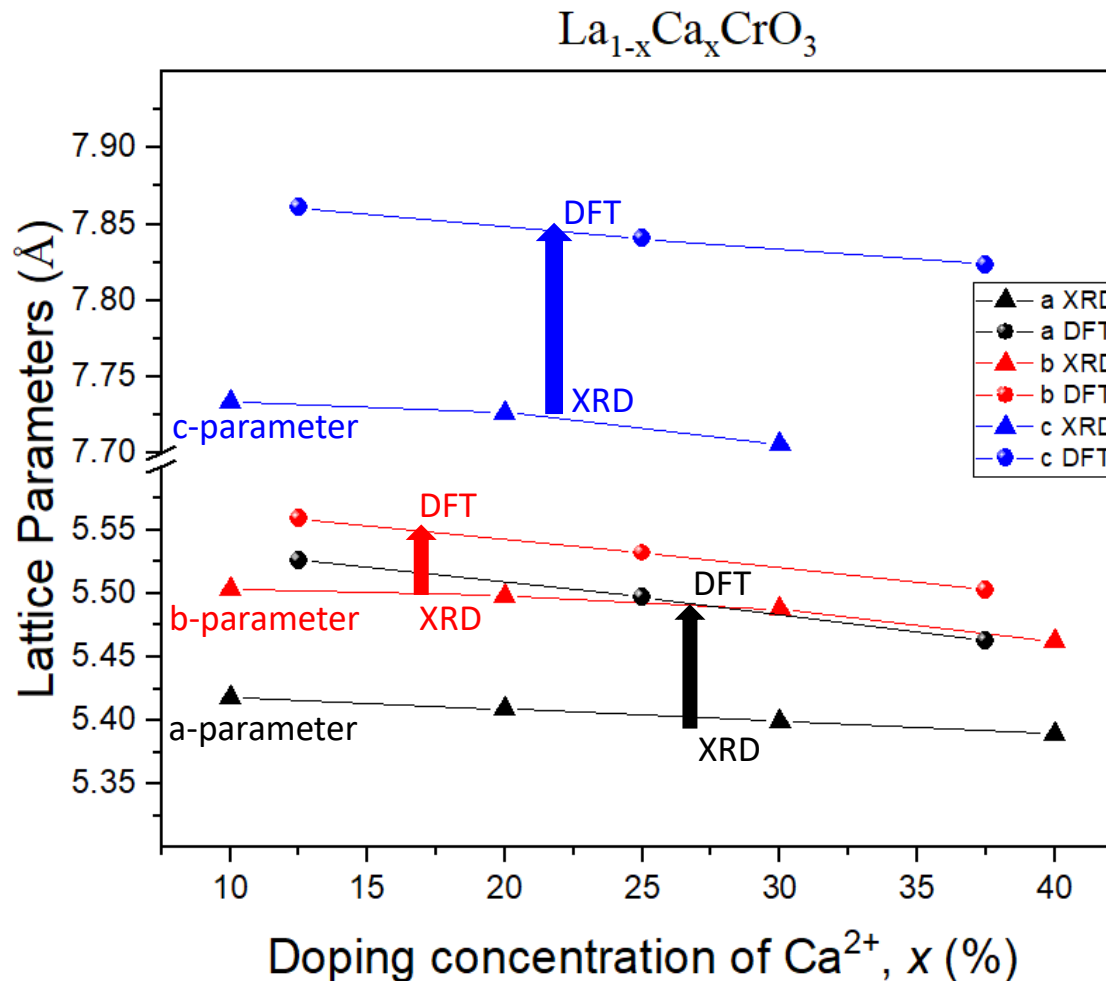
- ❖ Conductivity increase as function of doping level up to 30% for all dopants (strontium, calcium and manganese).
- ❖ At 40% doping levels conductivity decrease due to higher lattice distortion in all systems (solubility limit).
- ❖ Lower conductivity values under reducing atmospheres are explained by oxygen vacancies formation (near $>1.5\times$ in activation energy).

Computational Modelling for Ca-Doping Compositions

- ❖ First-principles spin-polarized calculation within the density functional theory (DFT) framework were performed.
- ❖ Calcium substitution levels used were 12.5%, 25.0% y 37.5%.
- ❖ Exchange and correlation effects were treated with generalized gradient approximation (GGA) and GGA+U. Vienna Ab initio Simulation Package (VASP) was used.
- ❖ A cutoff energy of 520 eV, and a $3\times6\times4$ k-point mesh was employed for a $2a\times1b\times1c$ $LaCrO_3$ orthorhombic supercell.
- ❖ The transport properties such as electrical conductivity (σ) was calculated using the BoltzTraP2 code that is formulated according to classical Boltzmann transport equation under the constant relaxation time (τ) approximation.

Work by: Victor Julio Mendoza Estrada (at Universidad del Norte)
Email: evictor@uninorte.edu.co

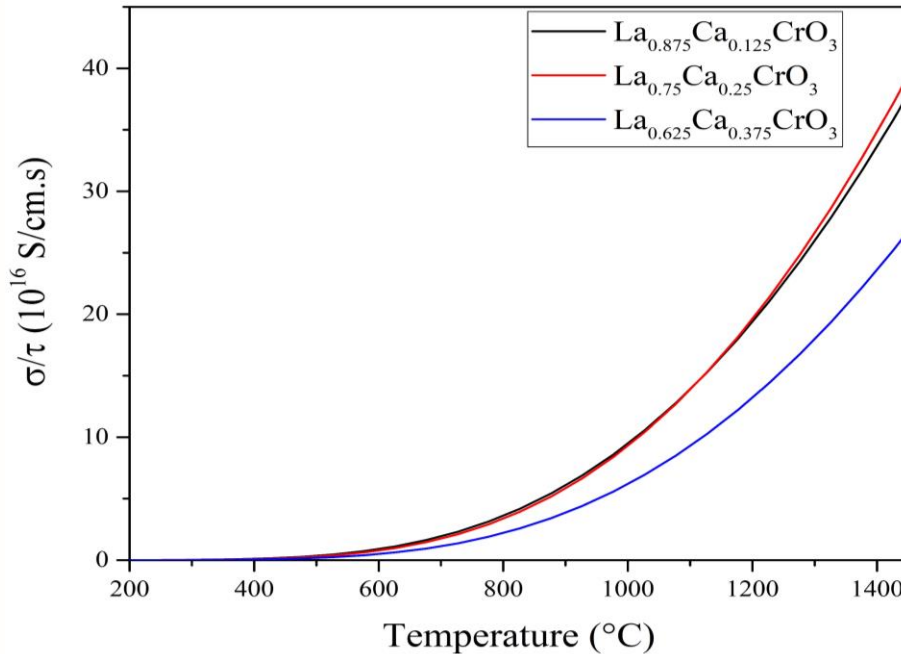
DFT and Experimental Lattice Parameters



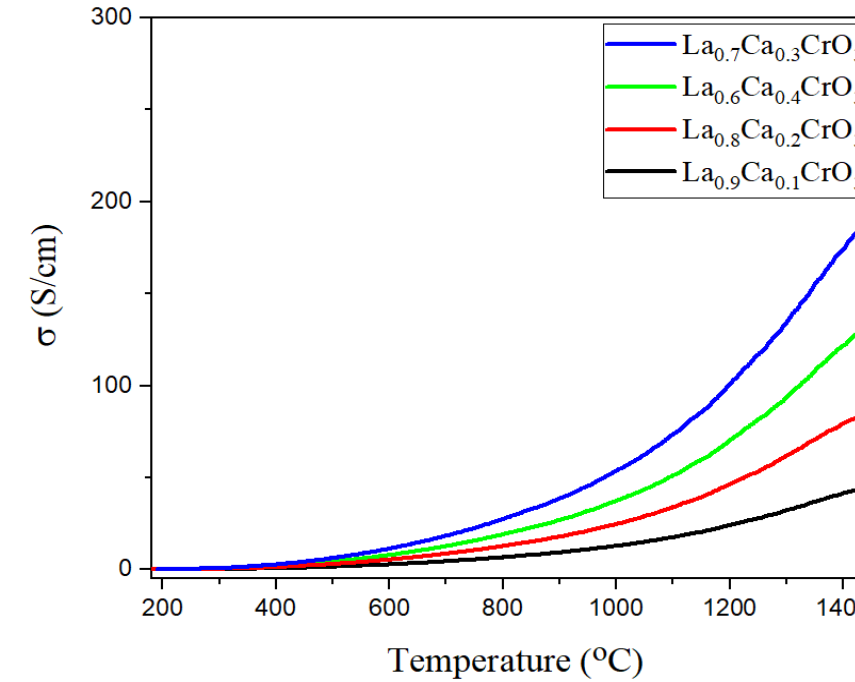
- ❖ Decrease in lattice parameters were observed when dopant cations are introduced in the lattice.
- ❖ To achieve neutrality chromium oxidation states, change from Cr^{+3} to Cr^{+4} , reduction in the chromium ionic size occurs.
- ❖ DFT theoretical data shows equal trends in the correlation between dopant level and lattice parameters as experimental data.
- ❖ DFT calculations of lattice parameters over-estimates lattice parameters values for all dopants and compositions in contrast with experimental XRD measurements.

Calculated Electrical Conductivity for Ca-Doping

DFT Results



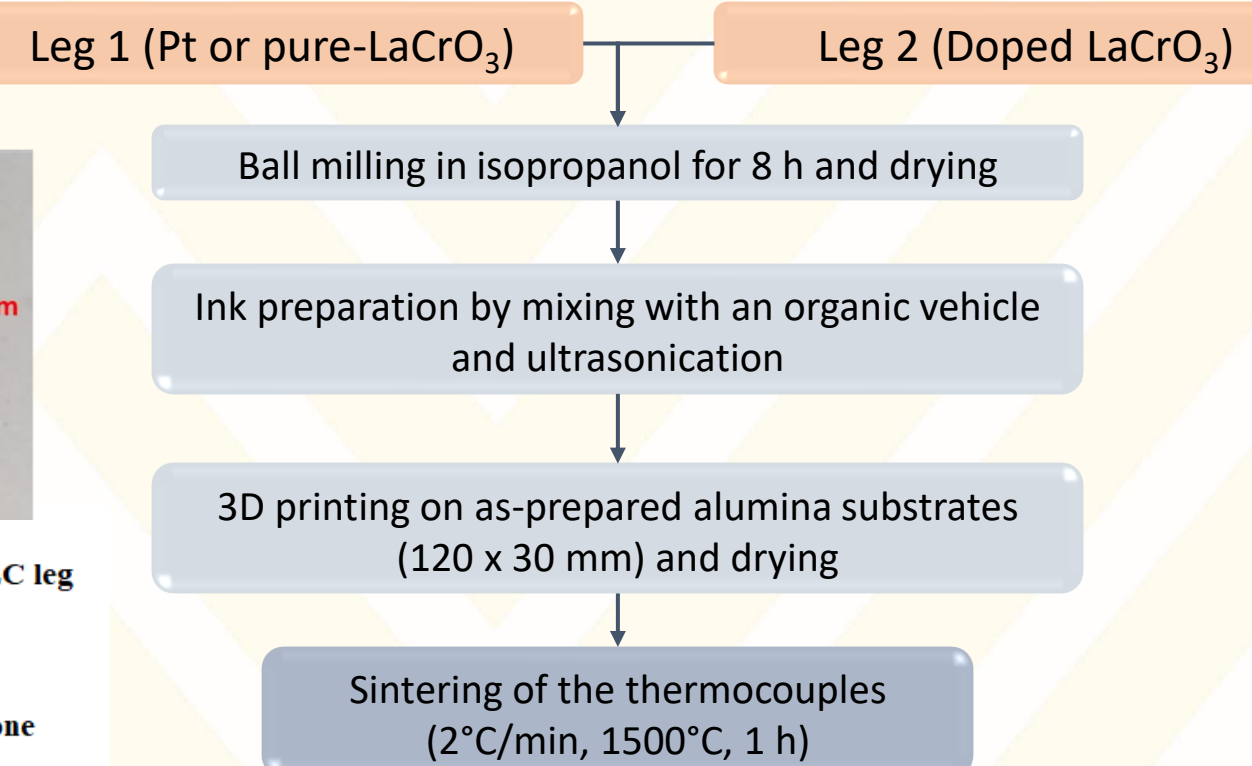
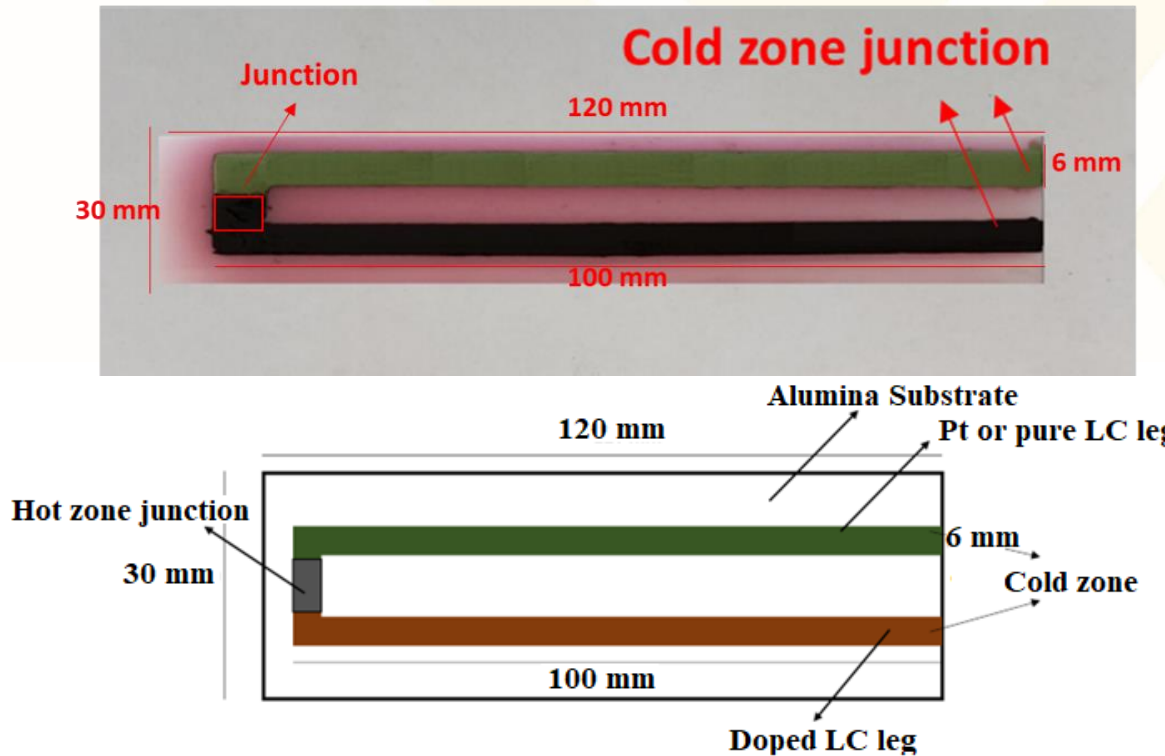
Experimental Results



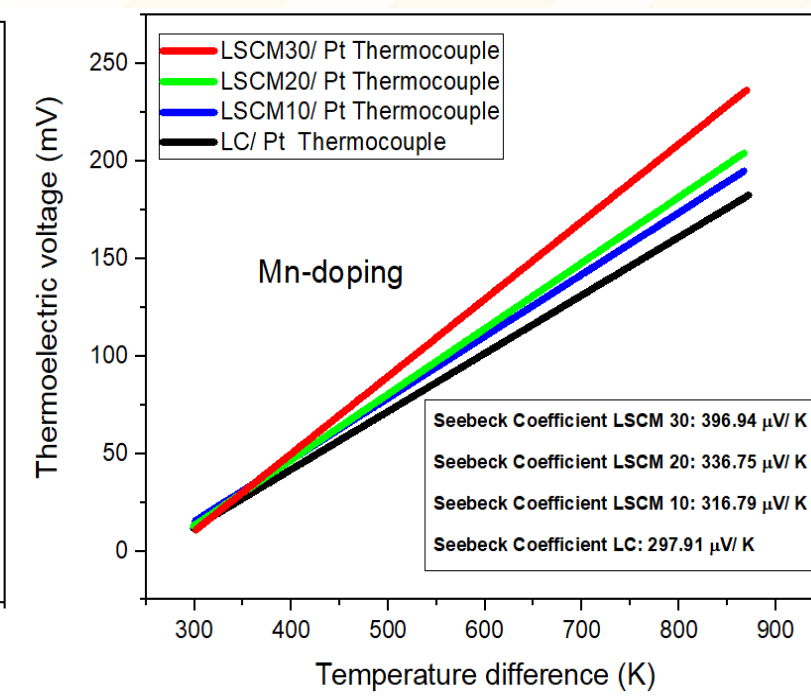
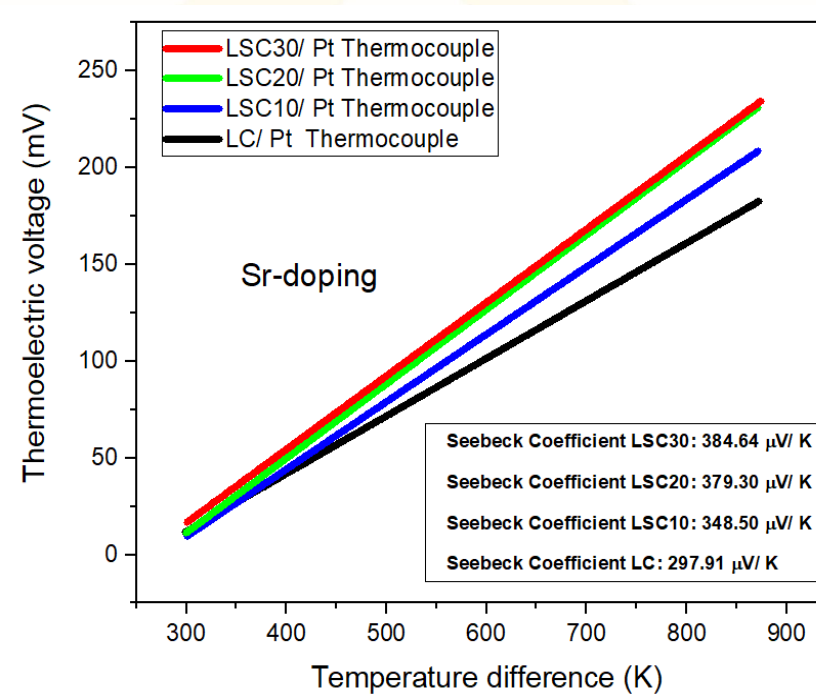
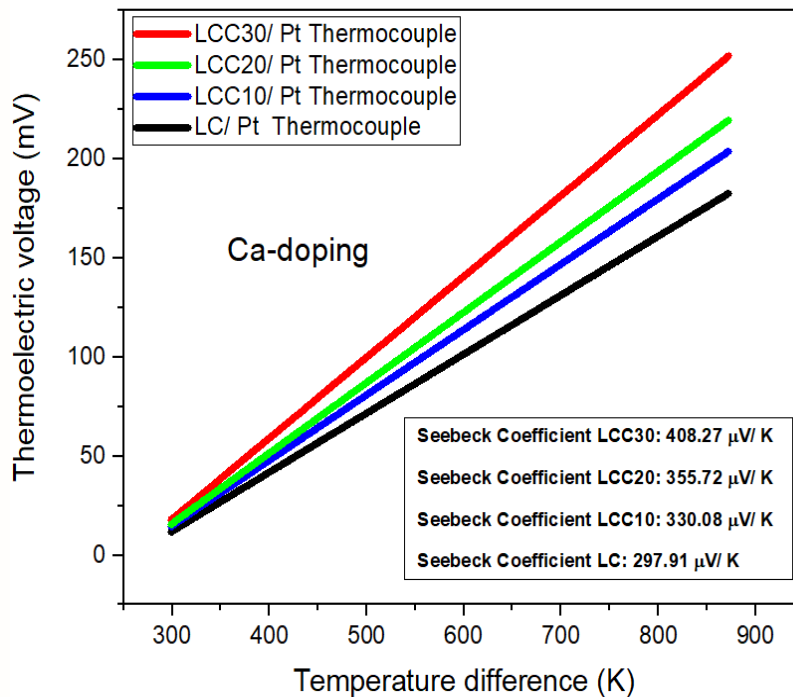
- ❖ The Ca-doped electrical conductivity presents proportional correlation increment with temperature, which is agreement with our experimental results.
- ❖ DFT calculated conductivity increase as a function of doping level up to 25% for calcium doping.
- ❖ DFT calculated conductivity dropped at 37.5% showing similar trend to 40% in experimental results.

High Temperature Thermocouple Fabrication

- Research team currently fabricating thermistors and thermocouples by (DIW) 3D printing.
- High-temperature thermocouples that function $>1200^{\circ}\text{C}$ (in R-type range) new exciting development.



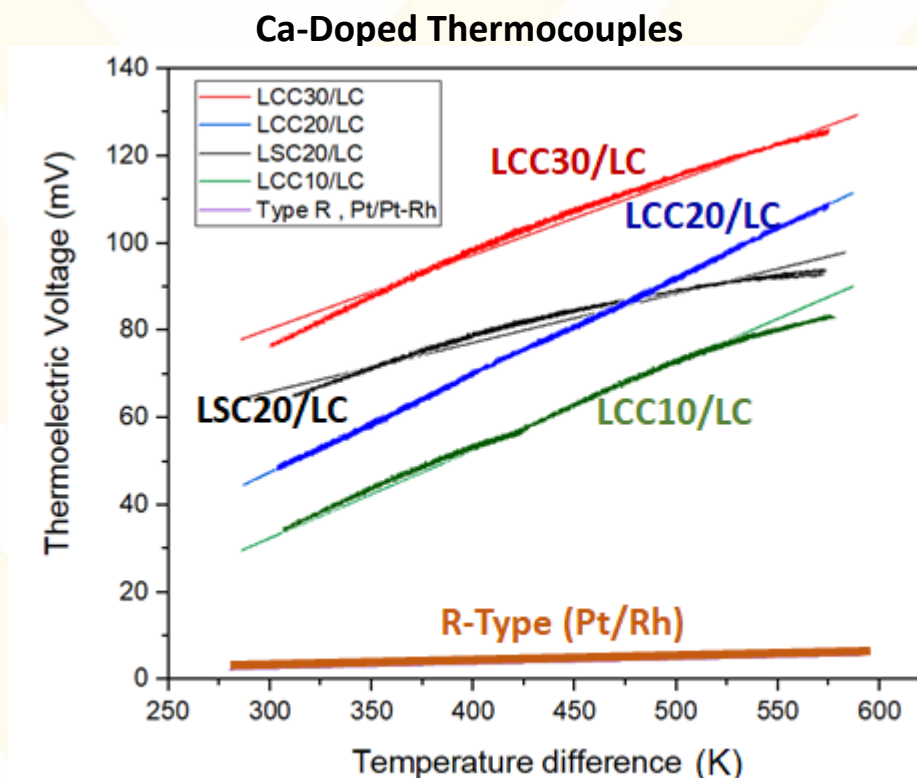
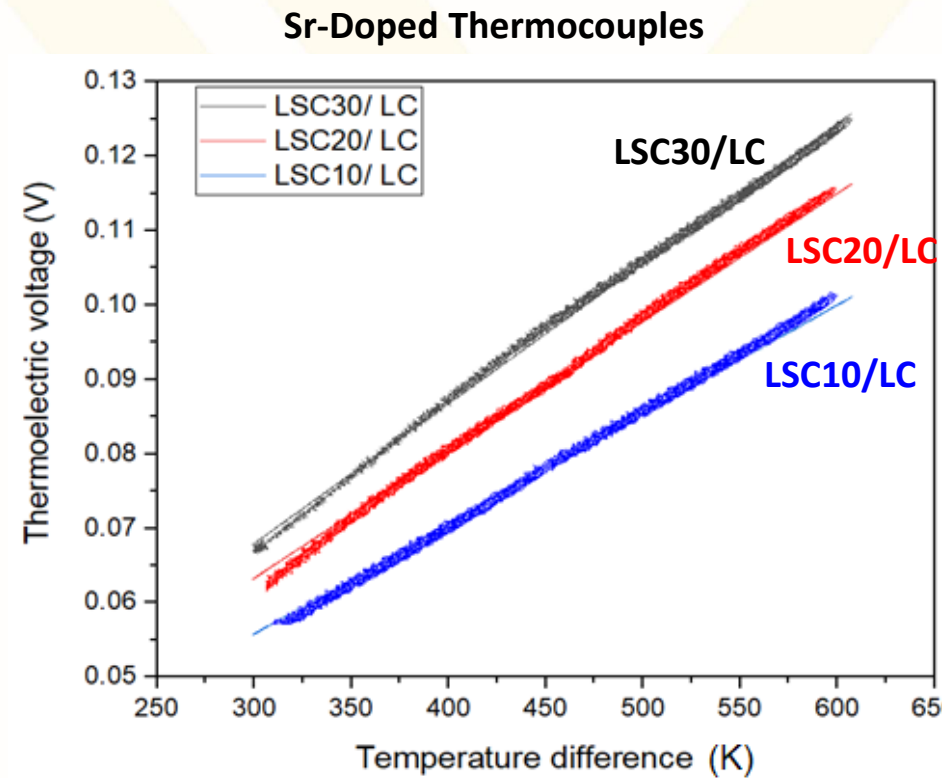
Seebeck Coefficient Estimation (Using Pt Standard)



- Linear correlation between temperature difference and thermoelectric voltage was observed for all the compositions.
- Doped- LaCrO_3 /Pt couples were fabricated to estimate absolute Seebeck coefficient ($S_{\text{Pt}} \sim -18 \mu\text{V}/\text{K}^*$) up to 1000°C.
- Ca doping shows highest absolute Seebeck coefficient (330-408 $\mu\text{V}/\text{K}$), with increasing Ca content.
- Ca doping on A-site has similar effect as Mn doping on B-site for LSC compositions.

*Moore, J. P. (1973). Journal of Applied Physics. 44 (3): 1174–1178

Thermoelectric Characterization of Thermocouples



- Thermocouples were tested in a range between 30 to 750°C during 3 heating cycles, showing an excellent reproducibility.
- Sr-doped compositions have lower Seebeck coefficient over Ca-doped compositions.
- The LCC30/LC, LCC20/LC and LCC10/LC thermocouples showed a maximum higher voltage by two orders of magnitude in comparison with Pt/Pt-Rh, with values of 124.61 mV, 116.50 mV and 80 mV respectively (at $\Delta T \sim 550^\circ\text{C}$).

Conclusions

- Using **Pechini Sol-Gel** method approach **high density (~96%)** doped lanthanum chromite compositions can be obtained. **Uniform phase** composition can be produced easily.
- **Lattice parameters reduce** proportionally with dopant content increment. **Divalent dopants produce** chromium oxidation state **changes** from +3 to +4 **reducing the ionic radius**.
- **Electrical conductivity** shows correlated **dependence** with high **temperature (up to 1500°C)** for all compositions. The exponential Arrhenius trend is evidence for the **polaron hopping electrical conduction** mechanism.

Conclusions

- Conductivity increase in function of doping level up to 30% for all dopants (strontium, calcium and manganese).
- Under reducing conditions conductivity decrease, chromium changes oxidation state from +4 to +3 and oxygen vacancies form to keep neutrality.
- Doping increases Seebeck coefficient and permits functional thermocouples to be fabricated with pure LaCrO_3 (showing thermoelectric voltages 2x greater than Pt thermocouples).

Acknowledgment

- ❖ We would like to thank **U.S. Department of Energy (DOE)** for sanctioning this project **DE-FE0031825**.
- ❖ We also would like to acknowledge Mr. Harley Hart, Dr. Qiang Wang, and Dr. Marcela Redigolo for their cooperation and valuable assistance in the WVU Shared Research Facilities (SRF).
- ❖ We also would like to thank HWI, for support us in developing real-life applications sensing systems/devices.
- ❖ Kindly acknowledge faculty and staff of West Virginia University for their support.



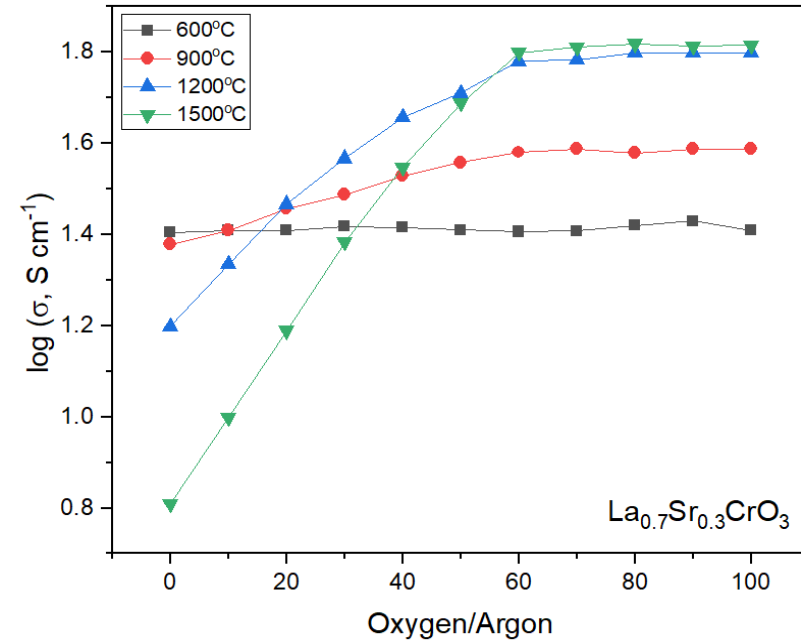
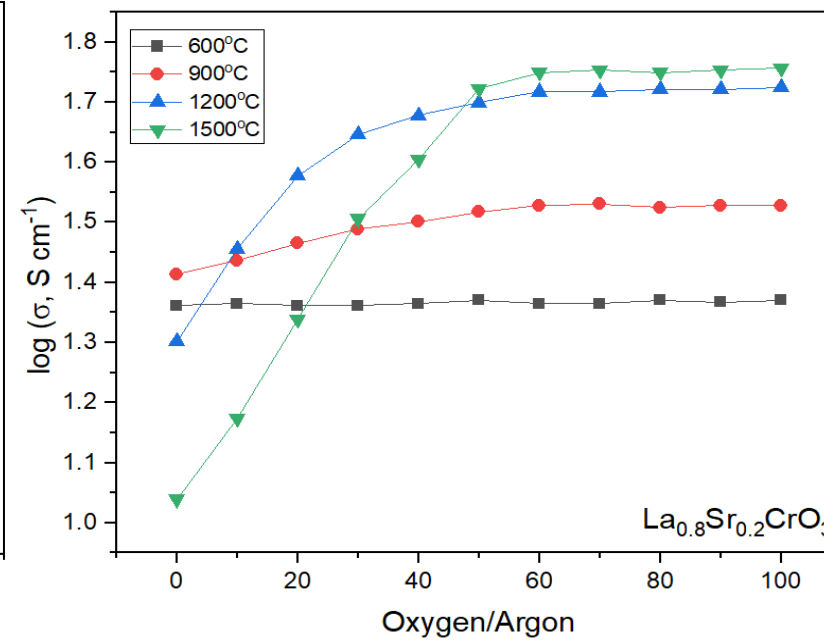
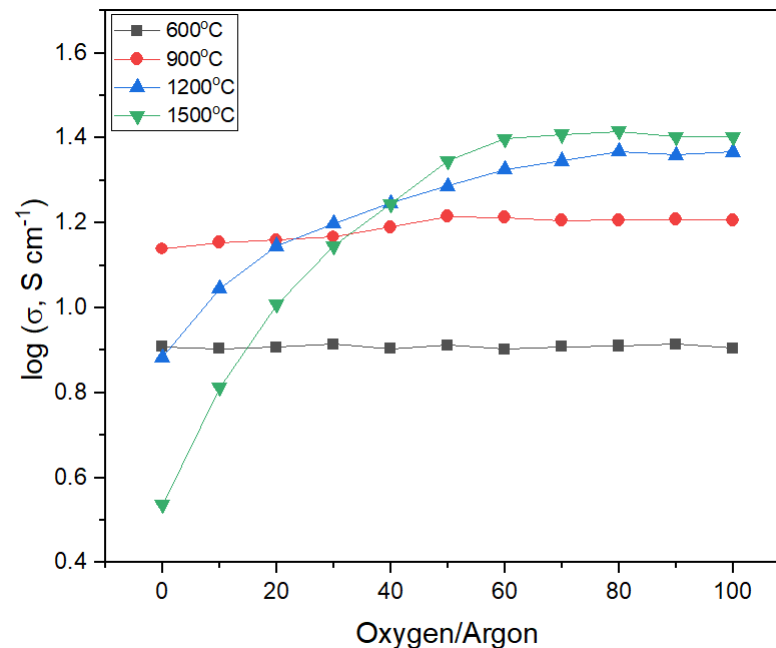
HarbisonWalker
International™



Thank you for the attention.

Email: jam0009@mix.wvu.edu

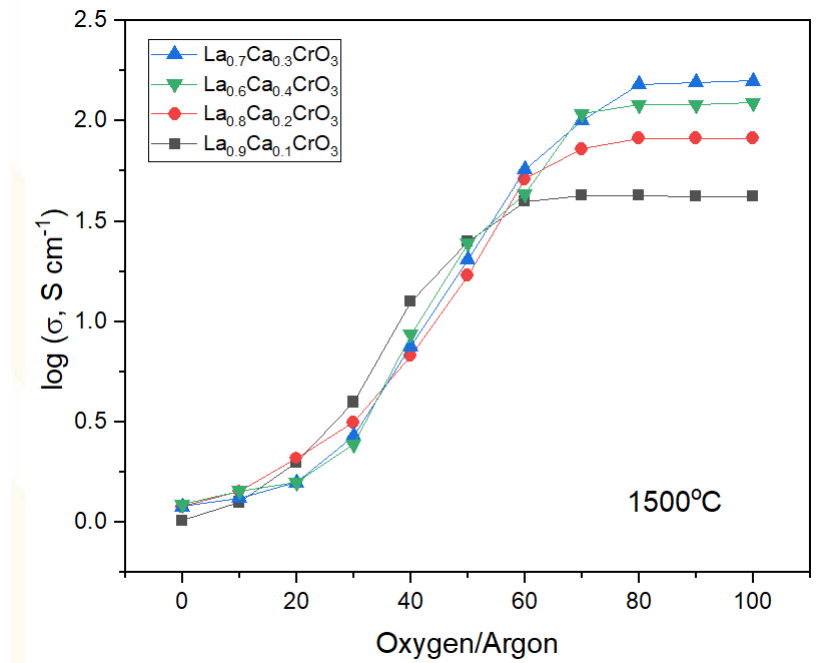
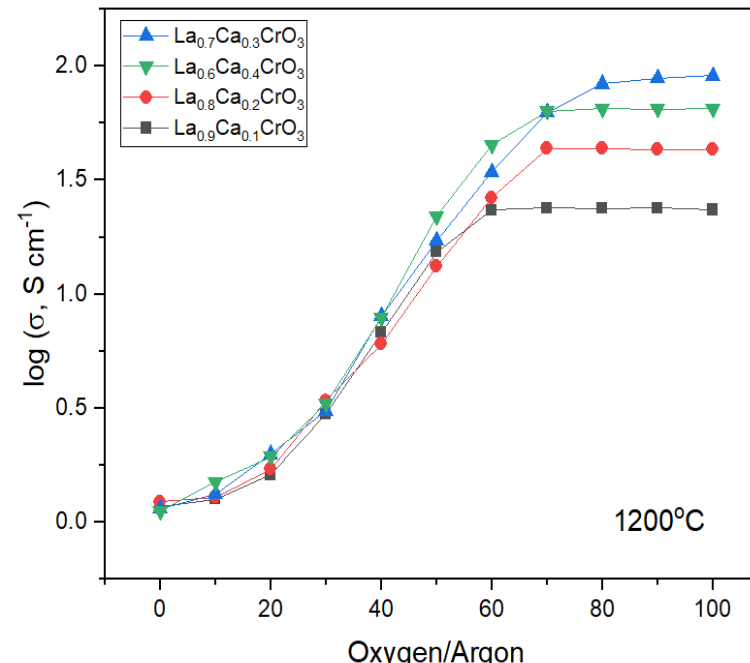
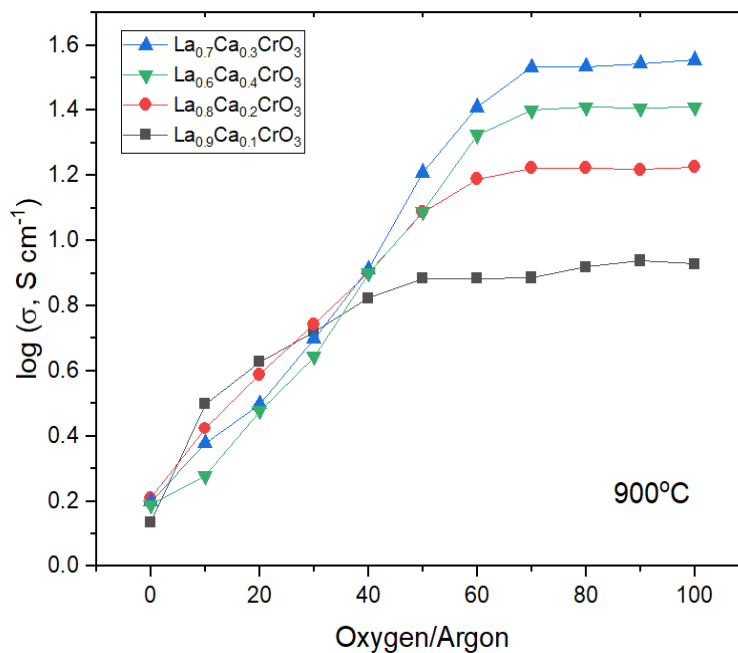
Electrical Conductivity (Oxygen partial pressure)



Electrical conductivity dependence of oxygen partial pressures at different temperatures for $\text{La}_{1-x}\text{Sr}_x\text{CrO}_3$

- ❖ At lower temperatures (600°C - 900°C) not significant changes in conductivity occurs for lanthanum doped compositions during the equilibrium time used (90 minutes).
- ❖ At higher temperatures (1200°C and 1500°C) the conductivity drops exponentially at lower oxygen partial pressures. Increasing the strontium concentration, the conductivity drop significantly.

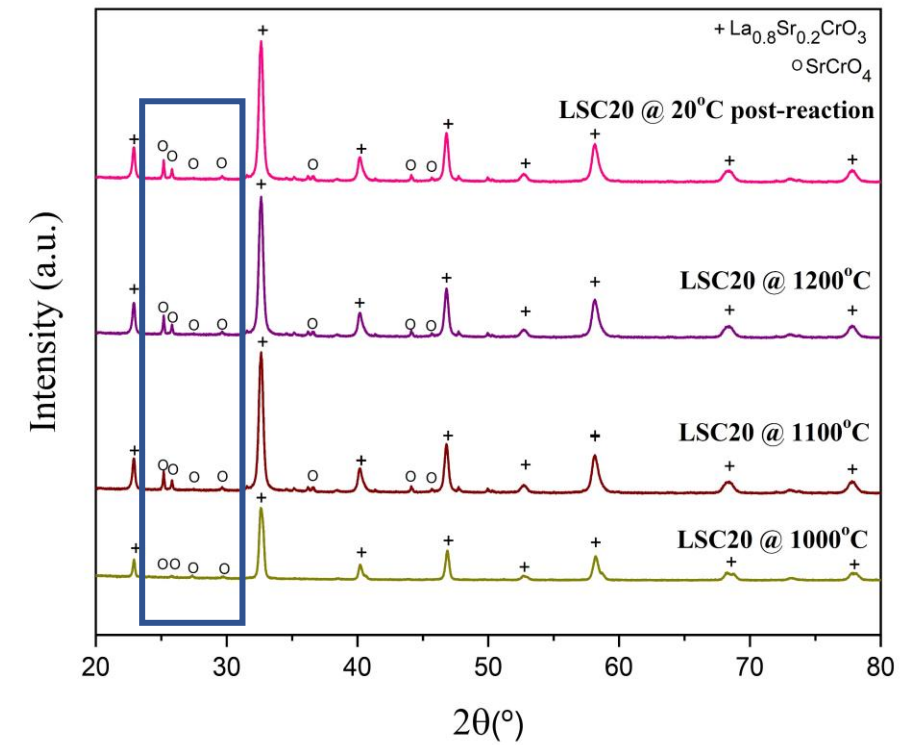
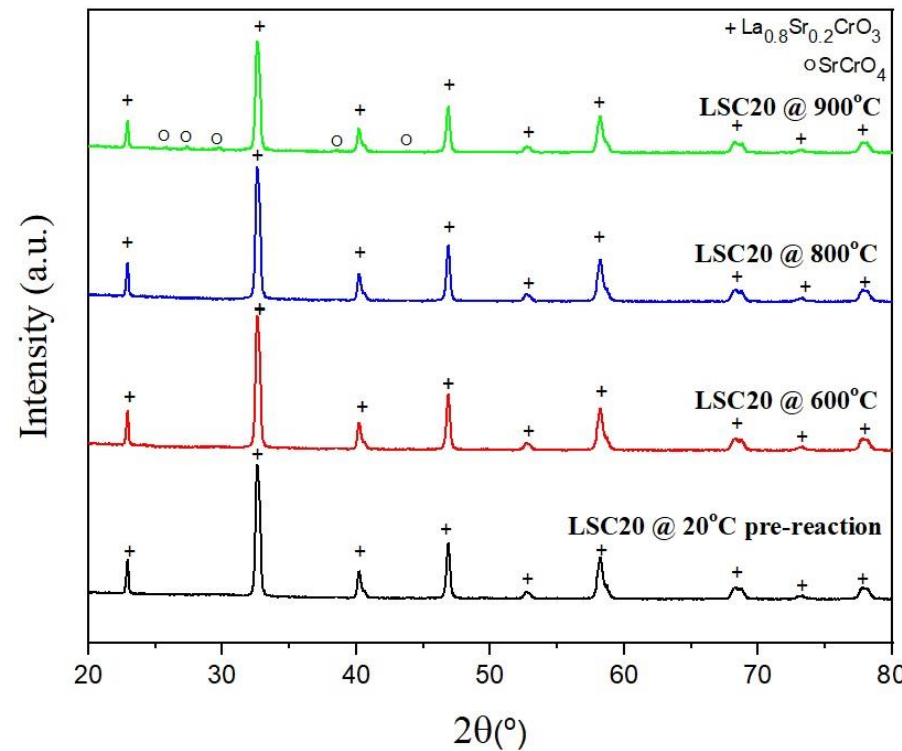
Electrical Conductivity (Oxygen partial pressure)



Electrical conductivity dependence of oxygen partial pressures at different temperatures for $\text{La}_{1-x}\text{Ca}_x\text{CrO}_3$

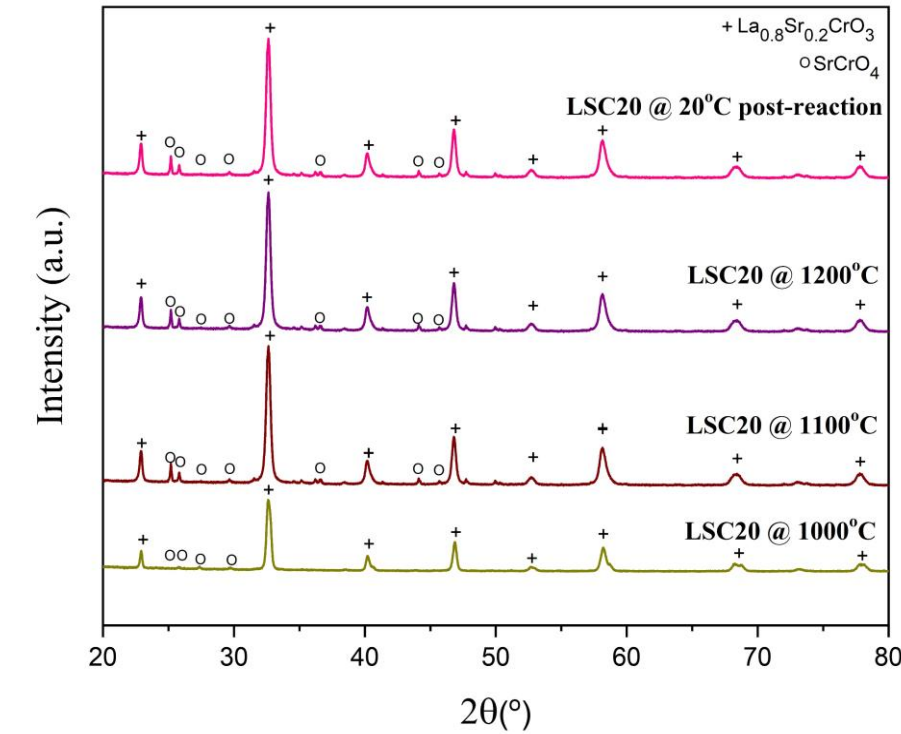
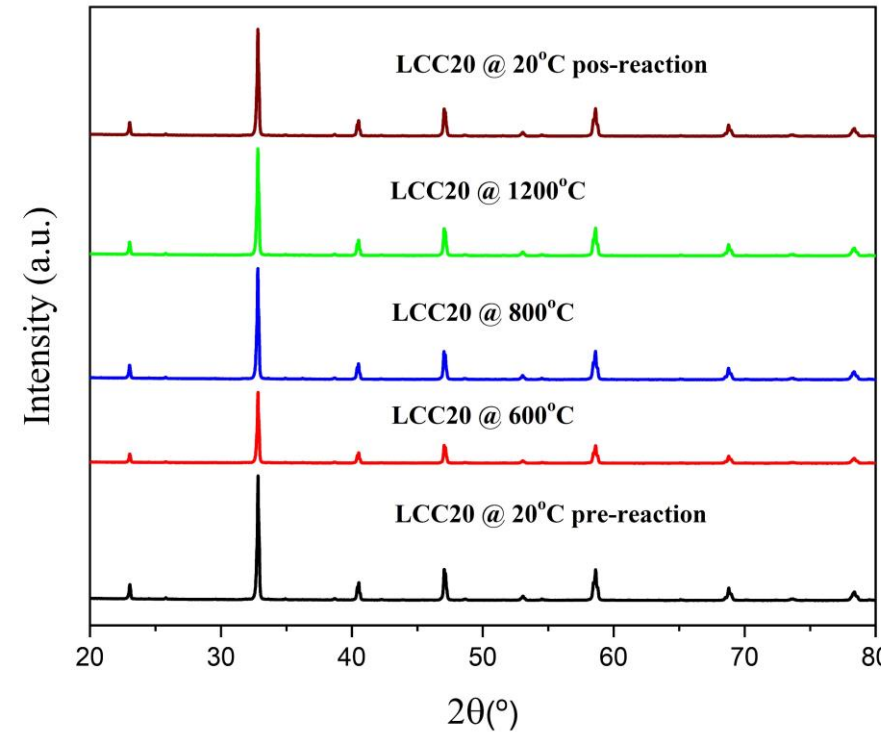
- ❖ When the oxygen partial pressure goes below a critical value, the oxygen vacancies are generated at expense of electron holes and conductivity decrease for all compositions.
- ❖ The charge imbalance caused by the introduction of Calcium starts to be compensated by the formation of oxygen vacancies.

Sr doped lanthanum chromite stability experiments



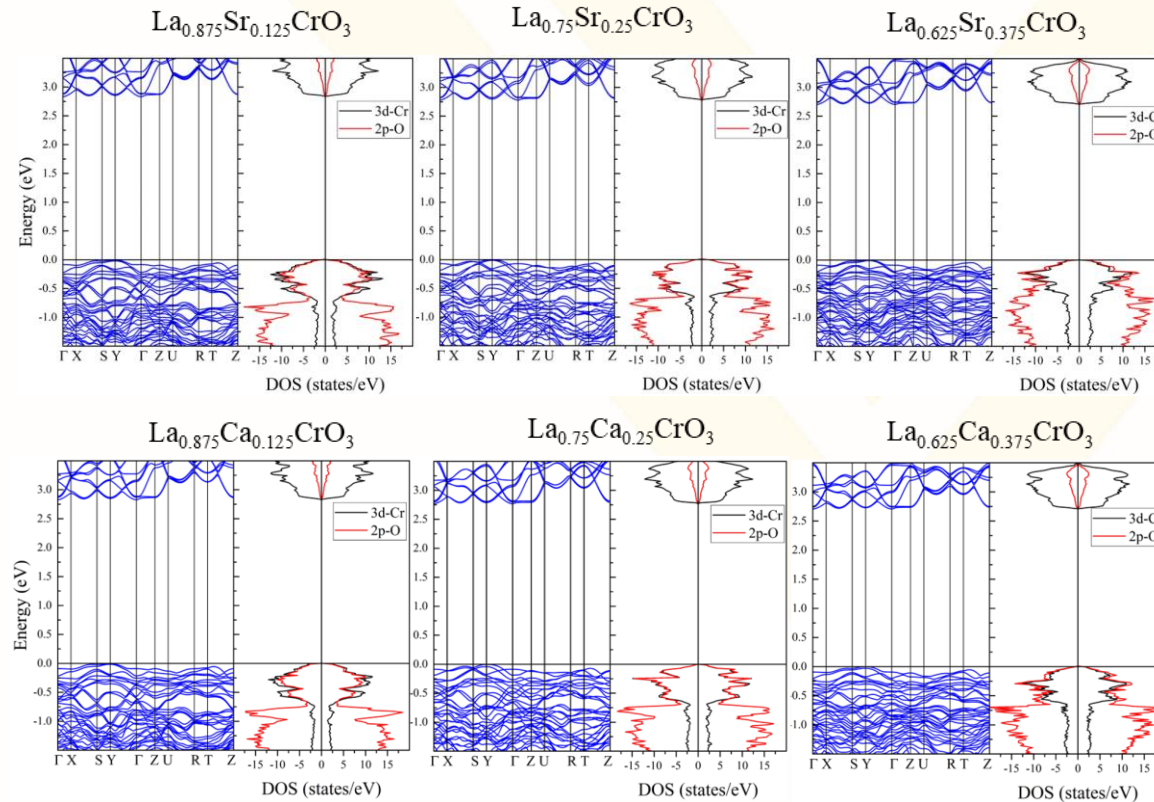
X-ray diffractograms of 20% strontium doped lanthanum chromite annealed at different temperatures.

Ca doped lanthanum chromite stability experiments



X-ray diffractograms of 20% strontium and calcium doped lanthanum chromite annealed at different temperatures.

Band structure and Partial Density of State (PDOS)



Band structure and PDOS for $\text{La}_{1-x}\text{Sr}_x\text{CrO}_3$ and $\text{La}_{1-x}\text{Ca}_x\text{CrO}_3$, $x = 0.125, 0.25$ and 0.375 with GGA+U ($U_{\text{eff-Cr}} = 3.3$ eV). The zero of the energy has been placed at the Fermi level, as indicated with horizontal black lines. In the PDOS, the values of the positive (negative) states correspond to the majority (minority) spin regions.

Band gap values for $\text{La}_{1-x}\text{Sr}_x\text{CrO}_3$ and $\text{La}_{1-x}\text{Ca}_x\text{CrO}_3$, $x = 0.125, 0.25$ and 0.375

Composition	Band Gap (eV)
LaCrO_3	2.908
$\text{La}_{0.875}\text{Sr}_{0.125}\text{CrO}_3$	2.836
$\text{La}_{0.75}\text{Sr}_{0.25}\text{CrO}_3$	2.783
$\text{La}_{0.625}\text{Sr}_{0.375}\text{CrO}_3$	2.710
$\text{La}_{0.875}\text{Ca}_{0.125}\text{CrO}_3$	2.827
$\text{La}_{0.75}\text{Ca}_{0.25}\text{CrO}_3$	2.772
$\text{La}_{0.625}\text{Ca}_{0.375}\text{CrO}_3$	2.706

- ❖ Band gap values decrease as a function of doping level for calcium and strontium content, and an insulating state was obtained for these structures which is in agreement with our experimental results.
- ❖ The symmetric distribution among the majority and minority spin regions in the PDOS of the both $\text{La}_{1-x}\text{Sr}_x\text{CrO}_3$ and $\text{La}_{1-x}\text{Ca}_x\text{CrO}_3$ explains the Antiferromagnetic behavior for these doped systems.